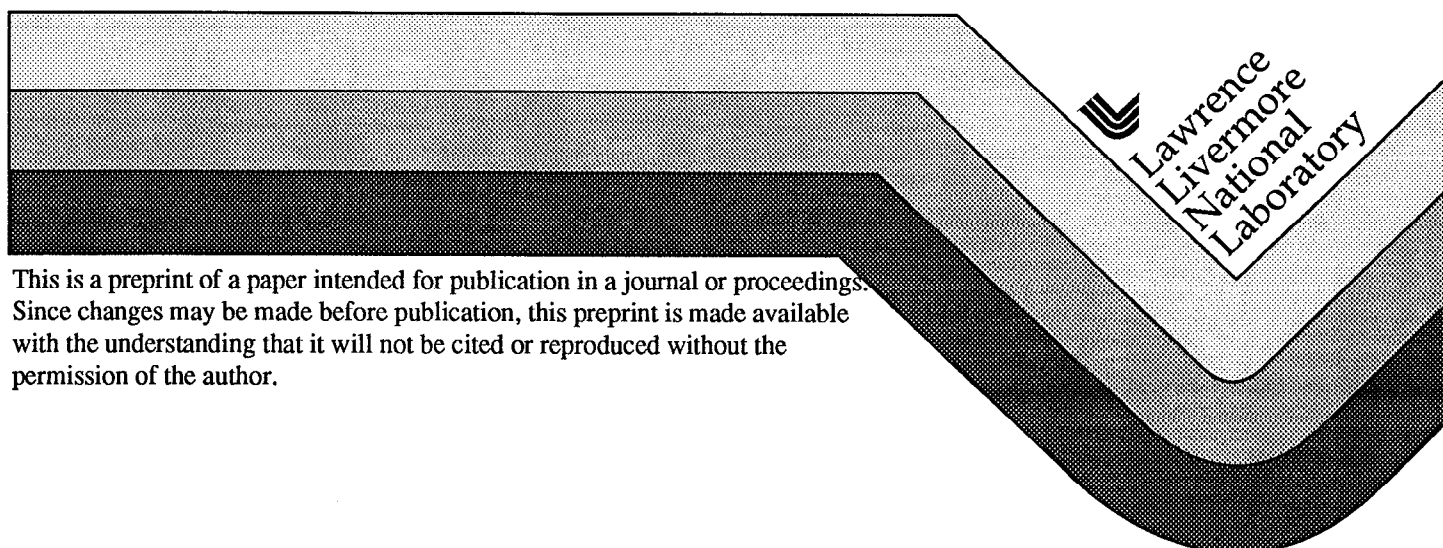


## Manufacture, Optical Performance and Laser Damage Characteristics of Diffractive Optics for the National Ignition Facility

J. A. Britten, S. M. Herman, L. J. Summers, M. C. Rushford, L. Auyang,  
I. M. Barton, B. W. Shore, S. N. Dixit, T. G. Parham, C. R. Hoaglan,  
C. T. Thompson, C. L. Battersby, J. M. Yoshiyama, and R. P. Mouser

This paper was prepared for submittal to  
30<sup>th</sup> Boulder Damage Symposium: Annual Symposium on Optical  
Materials for High Power Lasers  
Boulder, CO  
Sept. 28-Oct.1, 1998

December 15, 1998



#### DISCLAIMER

This document was prepared as an account of work sponsored by an agency of the United States Government. Neither the United States Government nor the University of California nor any of their employees, makes any warranty, express or implied, or assumes any legal liability or responsibility for the accuracy, completeness, or usefulness of any information, apparatus, product, or process disclosed, or represents that its use would not infringe privately owned rights. Reference herein to any specific commercial product, process, or service by trade name, trademark, manufacturer, or otherwise, does not necessarily constitute or imply its endorsement, recommendation, or favoring by the United States Government or the University of California. The views and opinions of authors expressed herein do not necessarily state or reflect those of the United States Government or the University of California, and shall not be used for advertising or product endorsement purposes.

# **MANUFACTURE, OPTICAL PERFORMANCE AND LASER DAMAGE CHARACTERISTICS OF DIFFRACTIVE OPTICS FOR THE NATIONAL IGNITION FACILITY**

J. A. Britten, S. M. Herman, L.J. Summers, M.C. Rushford, L. Auyang, I.M. Barton, B. W. Shore, S. N. Dixit, T. G. Parham, C. R. Hoaglan, C. T. Thompson, C. L. Battersby, J. M. Yoshiyama, R. P. Mouser

Lawrence Livermore National Laboratory,  
Livermore, CA 94550, U.S.A.

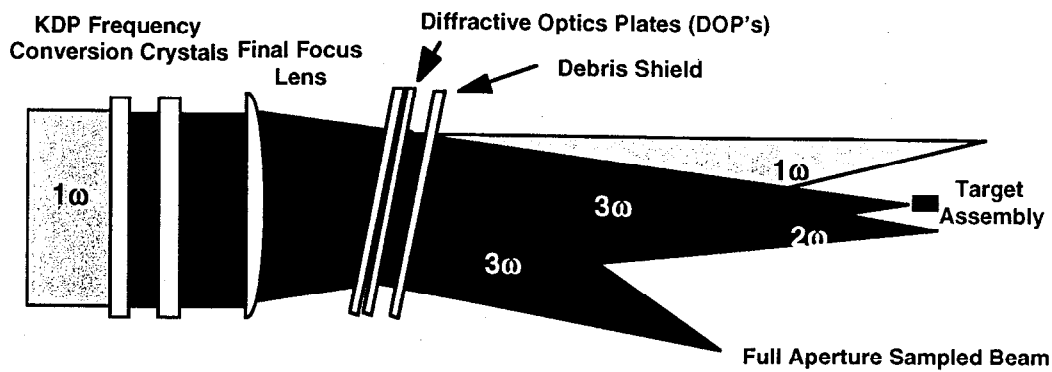
## **ABSTRACT**

We have fabricated demonstration diffractive optic plates (DOP's) at full scale for the National Ignition Facility (NIF) laser. These include an off-axis focusing beam sampling grating, a color separation grating, and a kinoform phase plate for spatial beam smoothing. Fabrication methods and optical performance of these DOP's are discussed. It was discovered that the sol-gel antireflective coating normally applied to high-power transmissive optics partially planarizes the diffractive structures, particularly on the color separation grating used for color management at target, to the extent that optical performance and laser damage threshold are negatively impacted. The effect of sol-gel coatings on grating performance, the feasibility of placing all diffractive structures on a single surface, and future work in this area are discussed.

**Key words:** Gratings, diffraction, antireflective coatings, wet etching

## **1. INTRODUCTION**

The NIF baseline laser design<sup>1</sup> incorporates three diffractive structures in the third harmonic (351 nm) final optics assembly, as shown in Figure 1. These include: 1) a beam sampling grating (BSG)<sup>2</sup> with focusing power that sends nominally 0.2-0.4% of the transmitted light into a calorimeter for energy diagnostics; 2) a color separation grating (CSG)<sup>3</sup> that transmits with high efficiency third harmonic light to the target while redirecting the unconverted first and second harmonic light away from the target with high rejection in the zero order, and 3) a kinoform phase plate (KPP)<sup>4</sup> that smooths the beam within a supergaussian envelope with a tailored spot size at the target plane. These optics are nominally 40 cm square aperture, and to withstand the design fluence, the patterns comprising the diffractive structure must be etched into the bulk fused silica substrate.



NIF uses three types of diffractive optics:

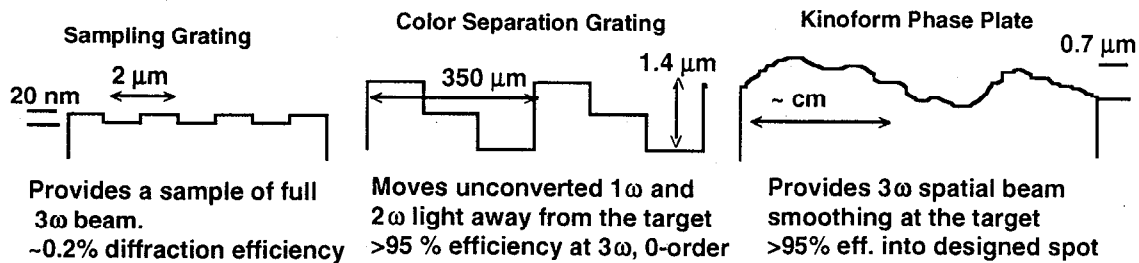


Figure 1. Schematic of NIF final optics assembly, showing the location, element geometry and specifications of the diffractive optics.

A flowchart of the processing steps used to manufacture these optics is shown in Figure 2. The BSG is a lamellar grating with a nominal period varying from 1-3  $\mu\text{m}$  and a modulation depth of approximately 20 nm. It is made holographically, by projecting two interfering coherent spherical waves onto the photoresist coated substrate in the appropriate geometry. One beam simulates the main beam going to target focus and the other the sampled beam focusing to a calorimeter. The latent image is developed to give a grating mask in resist. This pattern is transferred to the substrate surface by etching the exposed areas between the resist grating lines with a buffered hydrofluoric acid (HF) solution. The CSG is a stairstep grating design<sup>5-7</sup> made by proximity printing one line of the period through a chrome-on-quartz master mask onto a photoresist layer on the target substrate, developing this pattern and transfer etching with HF solution to a precise depth equal to one wave of optical phase difference in transmission at the use angle and wavelength. This process is repeated with the second line of the period by use of the same mask (or a different one) offset laterally relative to the first line etched. The KPP is similarly made with a 4-mask process with transfer wet etching<sup>4</sup> to produce 16 step levels approximating continuous, irregular topography on a several millimeter length scale, with maximum optical path difference of 1 wave. We have chosen wet etching for several reasons: the low aspect ratio of these structures is conducive to this process; it is inherently spatially uniform due to the kinetic control of the dissolution<sup>8,9</sup>; and it is inexpensive to implement.

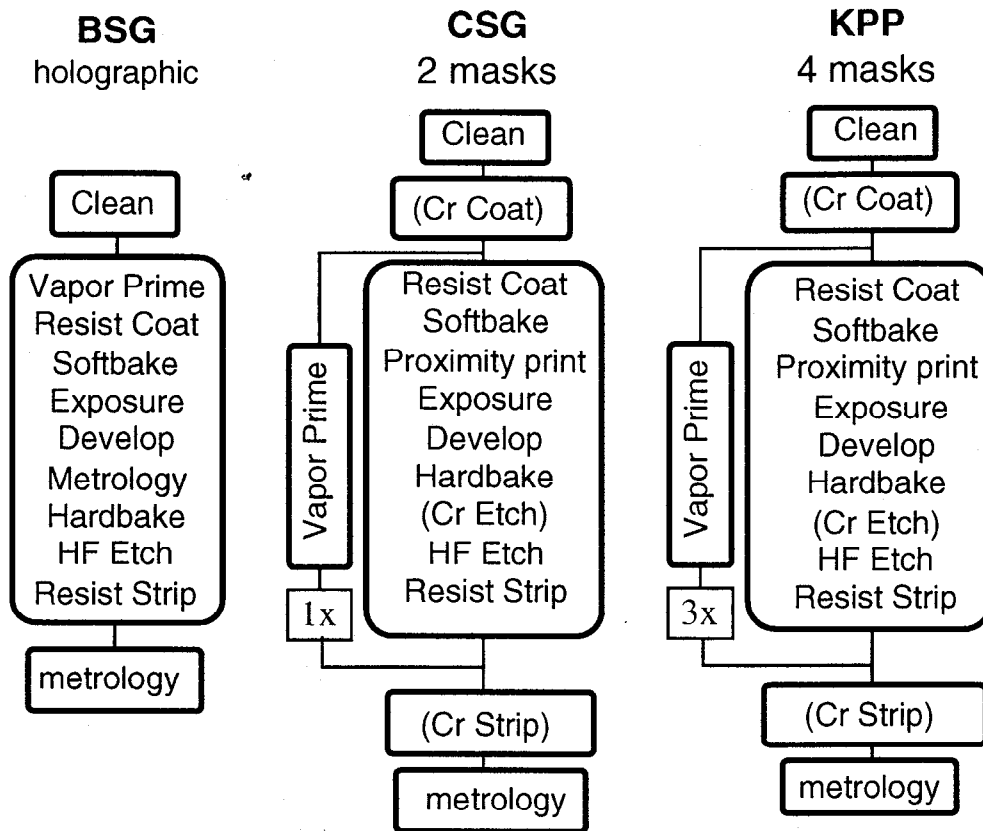


Figure 2. Flow diagram of processing steps required for fabrication of the three NIF  $3\omega$  diffractive optics.

We have constructed a facility at LLNL to manufacture DOP's onsite. This 2400 ft<sup>2</sup> facility became functional in January 1998. During the past year we have fabricated all three types of DOP at NIF scale, using custom-designed prototype processing equipment and manufacturing techniques that will be employed during full-scale production. Manufacture and performance of the BSG and CSG will be described. We have made and reported on several KPP's for LLNL's Nova laser and other laser systems<sup>4</sup> and the processing methods for these optics are identical to those of the CSG, so they will not be discussed.

## 2. BEAM SAMPLING GRATING

A laser interference lithography facility dedicated to fabrication of NIF BSG's has been constructed. The geometry of the exposure system is shown in Figure 3. A CW laser with a very long coherence length is required to generate stable, high-contrast fringes in the target plane. We use a 351 nm Ar ion laser because the wavelength very closely matches the third harmonic of the NIF. Thus, we can set up our exposure geometries identical to the deployment geometries in the NIF final optics assembly, and obtain a high-quality focal spot of the diffracted beam with minimal chromatic aberration of the

diffracted focus. The output of the laser in single-mode Tem00 operation is approximately 1.2 W. The exposure table is totally enclosed and vibrationally isolated using pneumatic supports. We also employ active fringe stabilization to ensure high pattern contrast. The major difficulty with this setup is in finding high-magnification objectives for the fast focus sampling beam that are suitable for transmitting 351 nm light. These are multi-element objectives that, in all objectives tested to date, imprint some degree of modulation onto the fringe pattern due to defects within the multi-element structure that are difficult to clean and entirely eliminate by spatial filtering.

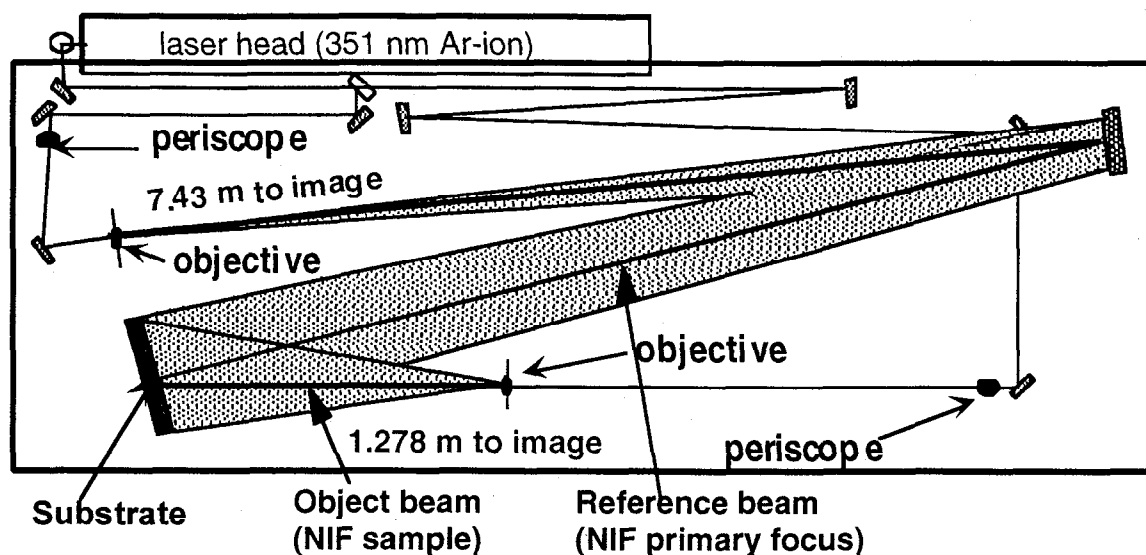


Figure 3. Schematic ofBSG holographic exposure geometry.

We have made demonstration BSG's on 41x39 cm fused silica plates using the process outlined in Figure 2. A map of the 1st order (focused) transmission efficiency of one such grating is shown in Figure 4. This measurement was made at 351 nm with the optic rotated 15 degrees about the vertical axis with respect to the incident beam, and the diffracted beam at an angle of 15 degrees above the horizontal axis of the optic. The mean efficiency of 0.37% is within specifications. The spatial uniformity needs to be improved upon, although model simulations giving the projected uncertainty of the spatial intensity variations of a NIF beamline suggest that this level of nonuniformity will not contribute to the measurement error. The efficiency variation results from a nonuniform grating linewidth, not an etch depth variation. The modulation seen in the diffraction efficiency is directly attributable to intensity variations in the spatially filtered sample writing beam, using a 40X objective. Improvements to this uniformity will be possible with higher quality objectives.

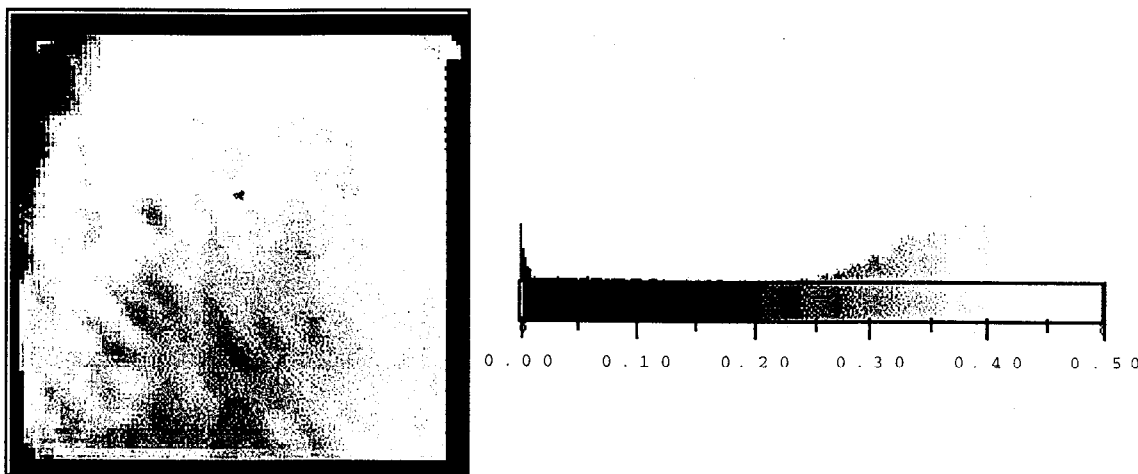


Figure 4. Diffraction efficiency (%) at -1 transmitted order for 351 nm at 14° incidence angle. BSG manufactured on a 41x39 cm diameter fused silica substrate. Mean efficiency is 0.37% with a standard deviation of 0.07%.

### 3. COLOR SEPARATION GRATING

Several CSG's have been fabricated and subjected to optical performance testing. The mask for these gratings was made by LLNL's laser plotter. It consisted of alternating 113 micron wide clear lines separated by 232 micron wide chrome spaces, 370 mm long, repeated over a 380 mm field. This pattern was printed on a 65 cm diameter fused silica substrate. The mask was printed pixel-by-pixel by positioning a 113x500 micron wide aperture with sub-micron accuracy, and using a shutter and beam smoothing optics, exposing the mask, previously coated with an evaporated chrome layer and then a photoresist layer, to light from a 413 nm Kr-ion laser. The pattern was transferred to the mask by subsequent developing of the resist and etching of the exposed chrome.

Target substrates, coated with chrome and then resist, were exposed to output from a collimated Hg lamp through this mask. They were then developed, hardbaked, chrome-etched and HF-etched to a depth of 357+/-10 nm to make the first step. The entire process was repeated with the mask shifted 114+/-1 microns laterally with the aid of fiducial marks on the mask and substrate viewed through confocal microscopes on the mask aligner, to etch the second step and double the depth of the first step. Undercutting (edge erosion) of the chrome and fused silica edges by 1-2 microns during this process was accounted for by undersizing the open area of the master mask. The end result was stairstep gratings repeating across the clear aperture of the 41x39 cm substrate, with a period of 345 microns.

A map of the zero-order transmission efficiency of one CSG at 351 nm and 13° incidence angle is shown in Figure 5. The average efficiency was 90.5%. This optic had no antireflective coating, so the theoretical efficiency accounting for Fresnel losses is 92.5%.

The additional losses, about 2%, are distributed in many higher transmitted orders. The zero order transmission of this optic at 527 and 1053 nm is 0.05 and 0.26 %, respectively, which exceed NIF specifications. We have made several such gratings with similar results.

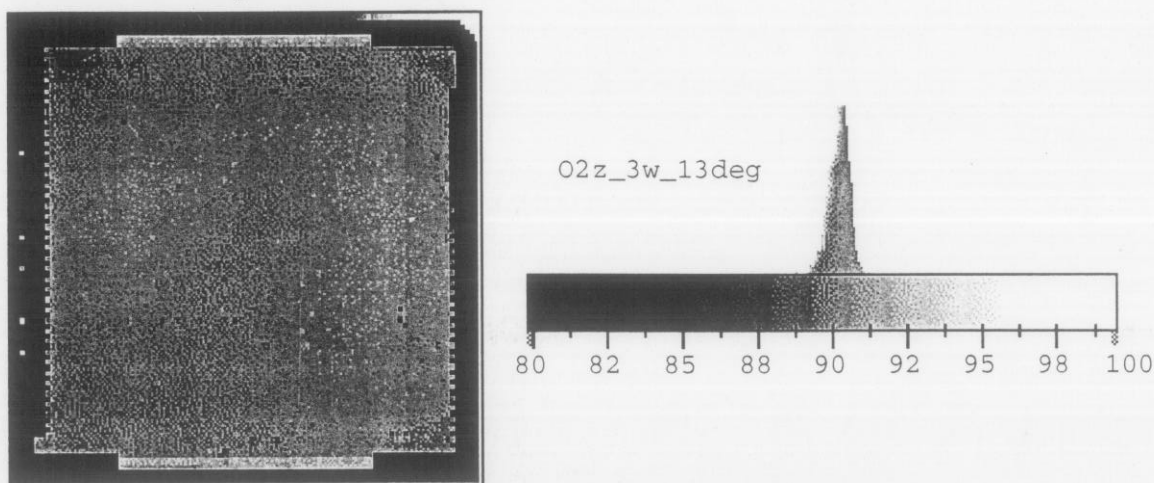


Figure 5. Zero-order transmission efficiency at 351 nm for a 41x39 cm CSG (#O2Z) at 13° incidence angle. Mean efficiency = 90.5% with  $\sigma = 0.75\%$ . Zero order transmission efficiencies at 1 and 2 $\omega$  were 0.26 and 0.05%, respectively. Both surfaces uncoated.

#### 4. EFFECTS OF SOL-GEL ANTIREFLECTIVE COATINGS

##### 4.1 CSG's

Transmissive optics for LLNL's high-power lasers have for years been coated with a high-damage resistant sol-gel colloidal silica antireflective (AR) film<sup>10</sup> applied by dip coating. Table 1 gives the zero-order 351 nm diffraction efficiency of a NIF-sized CSG that had such a coating applied, and then removed in places from the grating side and the back side by gentle wiping with a wet soft cloth. The highest efficiency is obtained with the AR coating removed from the grating surface. When the AR coating is on the grating surface, the reduction in back reflection is more than compensated for by an increase in efficiency in the higher transmitted orders. Thus, the 0-order transmission efficiency drops.

Table 1. Average zero-order transmission efficiency of NIF-sized CSG (#MDT) in areas approximately 10x38 cm in area where sol-gel AR dip coatings were either present or absent on grating and/or back surface.

	Both sides bare	AR coat back side	AR coat both sides
0-order transmission @ 351 nm (%)	90.8	93.5	89.6

This drop in transmitted 0-order efficiency is due to partial planarization of the etched structures by surface tension effects during post-application drying of the coating. Recall that the transmission at 351 nm at zero-order is maximized when the etched structures are of the precise depth to give integral multiples of a wave of phase retardation between adjacent elements. Planarization of the AR coating significantly alters this relationship between adjacent steps. SEM's of bare and AR coated CSG steps of 1.4 and 0.7 microns (2-wave and 1-wave steps) are compared in Figure 6. The ideal edge for a wet-etched CSG step is a quarter circle of radius equal to the etched depth. The bare CSG steps shown closely approximate this ideal. The accumulation of colloidal sol-gel particles at the step edges, caused by capillary forces which pull liquid from adjacent areas while the coating is drying but still fluid, results in increased film thickness many microns away from the edge. In the immediate vicinity of the steps, the coating is sufficiently thick so as to craze due to shrinkage-related tensile stresses.

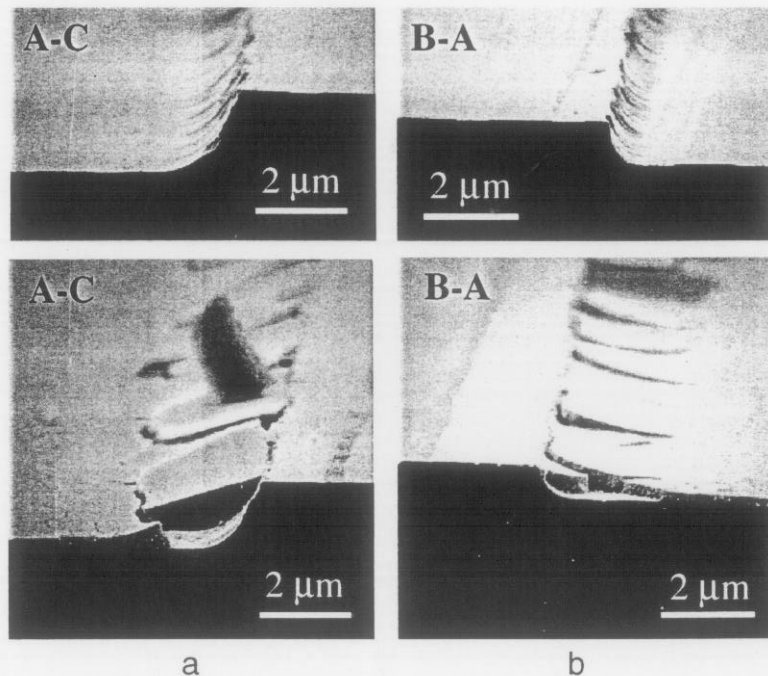


Figure 6. Scanning electron micrographs of CSG 2-wave (a) and 1-wave (b) steps wet etched into fused silica, bare (upper) and with a sol-gel AR dipcoat applied (lower).

As a consequence of this effect, sol-gel AR coated CSG's have significantly worse laser damage characteristics than when left uncoated. Modulation enhancement due to increased energy in high transmitted orders causes damage to downstream optics under conditions where normally minimal damage would be expected. Because of the extreme coarseness of the grating period with respect to the wavelength and the size of the beam, this modulation exists for several meters downstream where the orders overlap. An SEM of output surface damage caused by 351 nm, 7 ns irradiation of a NIF-sized AR dipcoated optic with a CSG pattern on the input surface is shown in Figure 7. This damage

was generated using LLNL's large-area damage tester<sup>11</sup>. The damage manifests itself as pinpoints that coalesce into lines correlatable to the grating period. Figure 8 shows the

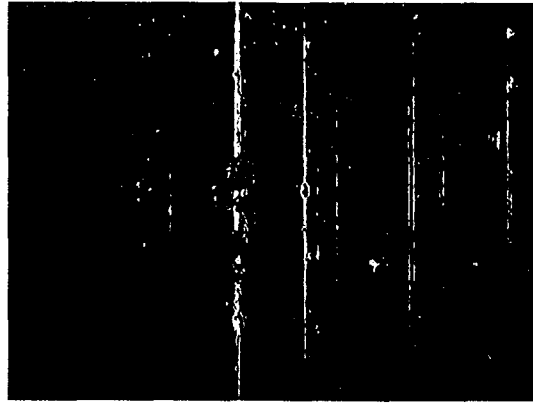


Figure 7. Micrograph of output-surface damage on fused silica caused by modulation from AR dipcoated CSG pattern on input surface illuminated with 351 nm light at 18 J/cm<sup>2</sup> from a 1.1 mm rastered beam at 7.5 ns<sup>11</sup>.

damage probability at 351 nm for the output surface of 5 cm diameter optics with CSG patterns on the input surface, with and without a sol-gel coating, as measured using LLNL's small-beam automated damage tester<sup>12</sup>. The damage probability is dramatically increased by the presence of a sol-gel dip coat. A spincoated sol-gel layer is more conformal than a dip-coated one, because capillary forces are not as dominant in this form of coating. Therefore, AR-coated CSG's applied by spinning exhibit lower modulation and less associated damage. However, these results are for small, round optics coated with a spin rate of about 2000 RPM. Due to its large size, spincoating of a NIF-sized part needs to be done at <1000 RPM. A lower spin rate results in greater planarization. Spincoated AR layers on large parts have exhibited significant and highly variable planarization effects which depend on spin rate, orientation of the grating steps, and position on the substrate. It has been concluded that sol-gel coatings deposited by either method on the CSG surface are unsuitable for NIF due to the likelihood of damage to downstream optics. An AR coating applied by vacuum deposition techniques would be largely conformal and not contribute to downstream modulation, but such coatings do not exist that can survive the NIF  $3\omega$  baseline fluence when applied to bare surfaces.

Work is currently underway to model and measure the modulation of bare and coated CSG's. The effect of bare edges as shown in Figure 6 is also being investigated, as any non-vertical edge will induce some degree of downstream modulation. The design for the NIF CSG is evolving toward using the natural dispersion of the focus lens to eliminate 1 and  $2\omega$  light from the target for all but the central portion of the beam. Here, a sub-aperture, uncoated CSG with a maximum allowable period (approximately 1 mm) will divert the 1 and  $2\omega$  light from the target. This design will minimize the area and density of etched steps and therefore minimize the modulation.

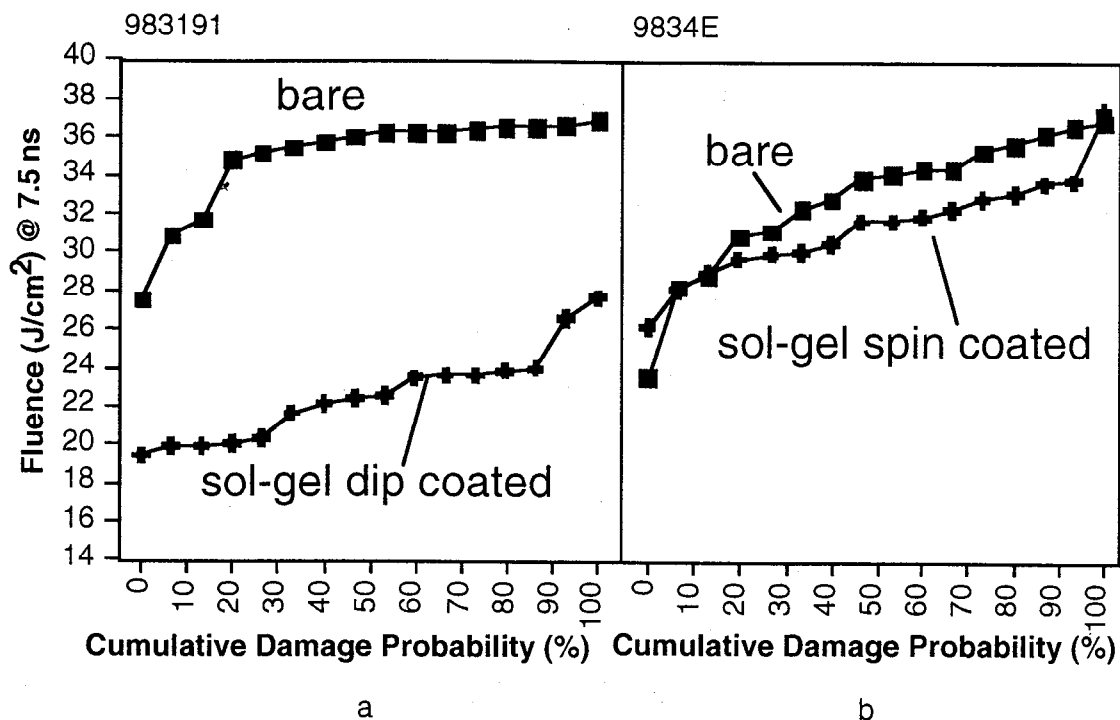


Figure 8. Cumulative damage probability -vs- fluence for output-surface damage with 345 nm period CSG on input surface, on 5 cm diameter fused silica windows, measured by LLNL's automated damage tester<sup>12</sup> at 351 nm, 7.5 ns. Plots show damage probability with input-surface grating either bare or coated with a sol-gel AR layer by dipcoating (a) or spincoating (b).

#### 4.2 BSG's

The BSG performance is influenced by AR coatings as well. The measured 1st order diffraction efficiency of one NIF-scale BSG changed from 0.4% bare to 0.15% after application of a dip-coated AR layer. The BSG structures are significantly shallower than the nominal AR coating thickness of 72 nm. Calculations predict that transmitted 1st-order diffraction efficiency drops by more than a factor of 3 when the grating is covered with a completely planar AR overcoat. It does not change if the coating is completely conformal. These situations are illustrated in Figure 9. These data imply that AR dipcoats atop BSG's are indeed largely planar. The diffraction efficiency of a BSG drops about 40% when the same sol-gel layer is applied by spincoating at approximately 2000 RPM, suggesting an intermediate degree of planarization. In the case of BSG's, this planarization does not increase the likelihood of laser induced damage, but the sensitivity of diffraction efficiency to coating characteristics raises the possibility that environmental changes to the coating can cause unacceptable changes to the diffracted efficiency. Work is underway to characterize experimentally and via modeling, the sensitivity of the diffraction efficiency of AR coated BSG's to environmental changes such as humidity and presence of condensable organic contaminants.


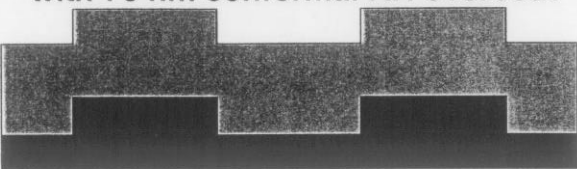
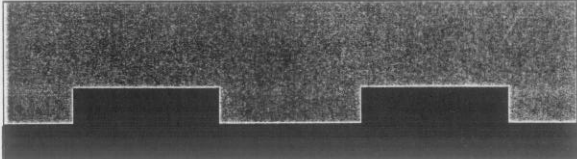
2 $\mu\text{m}$ period, 0.02 $\mu\text{m}$ depth 50% duty cycle etched grating	CALCULATED EFFICIENCY @ $3\omega$ (%)	
	-1 trans. order	$\Sigma$ (reflections)
	0.27	3.50
with 70 nm conformal AR overcoat		
	0.28	0.40
with 70 nm planarizing AR overcoat		
	0.08	0.20

Figure 9. Illustration of the calculated effect of sol-gel coating conformality on 1st order diffraction efficiency for a lamellar grating representative of the NIF baseline design for the BSG. At one extreme of conformality, there is no effect on grating efficiency, while at the other extreme of complete planarization, the efficiency is reduced by more than a factor of 3.

## 6. COMBINED DIFFRACTIVE STRUCTURES ON A SINGLE SURFACE

We have demonstrated the feasibility of combining the BSG and the CSG on the same surface<sup>13</sup> by the wet-etch process. The fine-featured BSG structures are formed first on a featureless substrate, then the CSG is made. Fabrication in the converse order (CSG followed by BSG) is problematic because planarization of the resist over the CSG topography would result in resist film thickness variations beyond the processing latitude of the holographic exposure technique used to write the BSG pattern.

Processing steps for both elements of the combined structure are the same as described earlier. Figure 10 shows CSG features profiled by white light interferometry and BSG features measured by atomic force microscopy. The measured optical performance of each diffractive structure is not affected by the presence of the other. The slight tapering of BSG profiles as they are propagated into the bulk during etching of CSG steps is predicted by models of isotropic etching<sup>13,14</sup>. These model calculations show that the nominal NIF BSG profile can be wet-etched approximately 4 microns deep before the grating ridges begin to lose height. Since the combined depth of a CSG/KPP is only at most 2.3 microns and fabrication methods for the KPP and CSG are the same, it would be straightforward to fabricate all three NIF diffractive structures on the same surface. This is an enabling development, since it may become important to concentrate all diffractive

structures onto one surface and leave it bare, in light of the problems that have arisen in finding a suitable AR coating for diffractive structures.

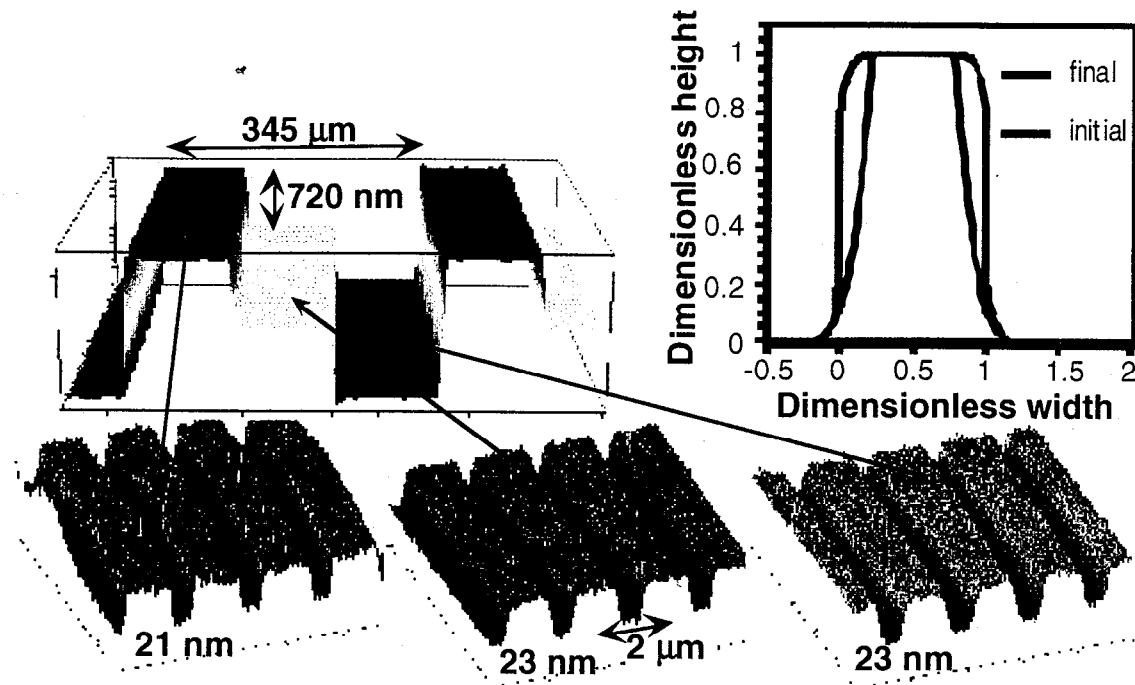


Figure 10. BSG profiles measured by atomic force microscopy on different CSG steps, which are imaged by white light interferometry. Initial grating aspect ratio (height/width) approximately 0.015. Upper right corner shows model calculations for initial and final BSG shape after etching to the depth of the deepest CSG structure.

## 7. CONCLUSIONS

We have fabricated demonstration diffractive optics required for the NIF baseline design at full-scale via wet-chemical etching of fused silica, using fabrication techniques and processing equipment suitable to large-scale production. We have examined the effect of AR sol-gel coatings on the performance and laser damage resistance of diffractive optics, and have concluded that the CSG must be left bare or stripped of the sol-gel coating to minimize modulation effects that will damage downstream optics. We have demonstrated the feasibility of combining all NIF diffractive structures onto a single surface.

## ACKNOWLEDGMENTS

This work was performed under the auspices of the U.S. Department of Energy under contract no. W-7405-Eng-48.

## REFERENCES

1. R. E. English, Jr., 'Overview of the NIF Optical System Design' Lawrence Livermore National Laboratory Rept. UCRL-LR-105821-97-3 (1997)
2. J.A. Britten, R.D. Boyd, M.D. Perry, B.W. Shore and I.M. Thomas, 'Low-Efficiency Gratings for Third-Harmonic Diagnostic Applications' Proc. SPIE **2633**, 1<sup>st</sup> Int'l. Conf. on Solid State Lasers for Application to Inertial Confinement Fusion, M. Andre and H.T. Powell, eds., 121-128 (1995)
3. S.N. Dixit, M.C. Rushford, I.M. Thomas, S.M. Herman, J.A. Britten, B.W. Shore and M.D. Perry, 'Color Separation Gratings for Diverting the Unconverted Light Away from the NIF Target', Proc. SPIE **3047**, 2<sup>nd</sup> Int'l. Conf. on Solid State Lasers for Application to Inertial Confinement Fusion, M. Andre ed., 463-470 (1996)
4. M.C. Rushford, S.N. Dixit, I.M. Thomas, A.M. Martin and M.D. Perry, 'Large-Aperture Kinoform Phase Plates in Fused Silica for Spatial Beam Smoothing on Nova and the Beamlet Lasers', Proc. SPIE **3047**, 2<sup>nd</sup> Int'l. Conf. on Solid State Lasers for Application to Inertial Confinement Fusion, M. Andre ed., 282-292, (1996)
5. H. Dammann, 'Color Separation Gratings', *Appl. Opt.*, **17**, 2273-2279, (1978)
6. M.W. Farn, M.B. Stern, W. B. Veldkamp and S.S. Medeiros, 'Color Separation by Use of Binary Optics', *Optics Lett.* **18**, 1214-1216, (1993)
7. T.H. Bett, R.M. Stevenson, M.R. Taghizadeh, T.M. Lightbody, P. Blair, B. Layet, N. Watson, I. Barton, G. Robb and J. McMonagle, 'Diffractive Optics Development for Application on High-Power Solid State Lasers', Proc. SPIE, **2633**, 1<sup>st</sup> Int'l. Conf. on Solid State Lasers for Application to Inertial Confinement Fusion, M. Andre and H.T. Powell, eds., 129-140, (1995)
8. G.A.C.M. Spierings, 'Wet Chemical Etching of Silicate Glasses in Hydrofluoric Acid Based Solutions', *J. Mater. Sci.*, **28** 6261-6273 (1993)
9. D.T. Liang and D.W. Readey, 'Dissolutions Kinetics of Crystalline and Amorphous Silica in Hydrofluoric -Hydrochloric Acid Mixtures', *J. Am Ceram Soc.*, **70** 570-577, (1987)
10. I. M. Thomas, 'High-Laser Damage Threshold Porous Silica Antireflective Coating', *Appl. Opt.* **25**, 1481-1483, (1986)
11. S. Schwartz, M. Feit, M. R. Kozlowski, R.P. Mouser and Z. Wu, "Current 3w

large optic test procedures and data analysis for the QA of NIF optics", This Proceedings (1998)

12. L. Sheehan, S. Schwartz, C. Battersbey, R. Dickson, R. Jennings, J. Kimmons, M. Kozłowski, S. Maricle, R. Mouser, F. Rainer, M. Runckel and Z. Wu, "Automated damage test facilities for materials development and production optic quality assurance at LLNL", This Proceedings, (1998)

13. J.A. Britten and L.J. Summers, 'Multiscale, Multifunction Diffractive Structures Wet-Etched into Fused Silica for High Laser Damage Threshold Applications', *Applied Optics*, **37**, 7049-7054 (1998)

14. S. Lindau, 'The Groove Profile Formation of Holographic Gratings', *Opt. Acta*, **29**, 1371-1381, (1982)